

Correction to “Molecular Simulations Indicate Marked Differences in the Structure of Amylin Mutants, Correlated with Known Aggregation Propensity”

Cayla Miller, Gül H. Zerze, and Jeetain Mittal*

J. Phys. Chem. B **2013**, *117* (50), 16066–16075. DOI: 10.1021/jp409755y

The horizontal axes in Figures 3 and 9 were incorrectly numbered in reverse order, from the C-terminal to the N-terminal end, while our interpretation followed the standard N- to C-terminal numbering. The corrected Figures 3 and 9 are shown herein. The major conclusions remain unaltered, as results in the original paper from free energies on RMSD from known NMR and X-ray crystal structures supported the importance of both regions 8–17 and 22–28, and long-range effects of mutations remain. Upon the basis of the renumbered Figure 3, we now find that the major difference in α -helical propensity between sequences, correlated with aggregation propensity, appears over residues 22–31.

The helical region identified over residues 22–31 coincides, in part, with the experimentally known amyloidogenic region 20–29, as well as with the region 22–28. In the original paper, over the latter region, we already performed RMSD from near-membrane amylin structures and found our hIAPP and hIAPP S20G trajectories to sample structures similar to those from membrane-mimicking environments, whereas neither rIAPP nor hIAPP I26P sampled similar structures. Furthermore, the renumbered Figure 9 shows that reduction of the disulfide bond in both human and rat amylin is associated with reduced α -helix propensity of the N-terminal residues, in agreement with experimental work cited in our paper, while β -sheet propensity of the N-terminal residues is increased. Long-range contacts appear to affect the secondary structure of C-terminal residues as well.

Additionally, the first and second columns in Figure 8 should be labeled “R_g” and “E2E,” respectively, and in-text references to said figure interchanged likewise. The conclusions remain the same, as qualitative trends in these lengths are unaffected.

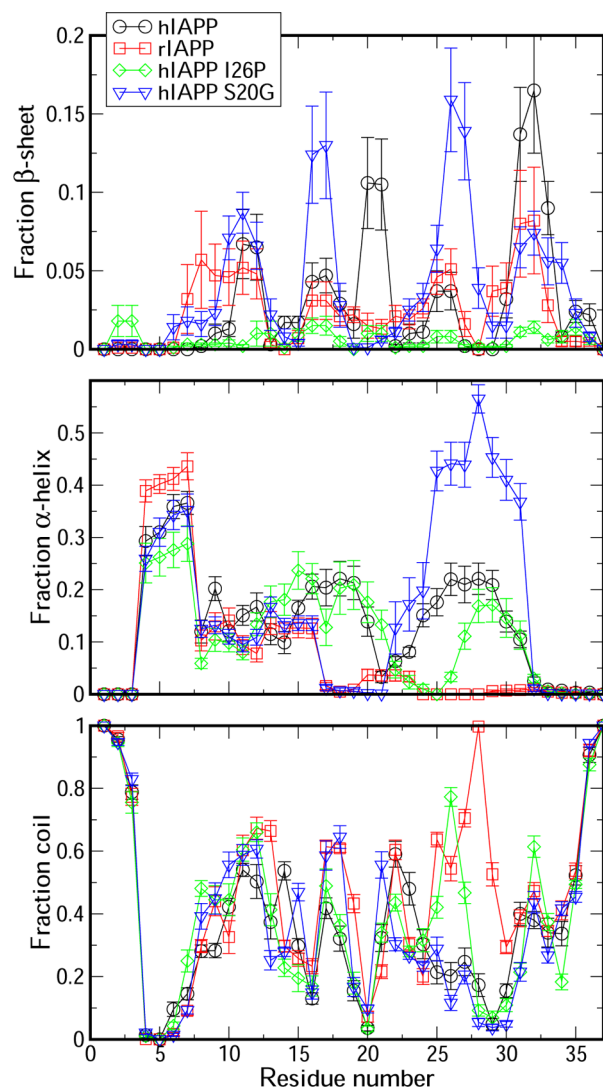


Figure 3. Per-residue fraction of time spent in secondary structure over the last 150 ns for wild-type hIAPP, rIAPP, hIAPP S20G, and hIAPP I26P.

Published: July 9, 2014

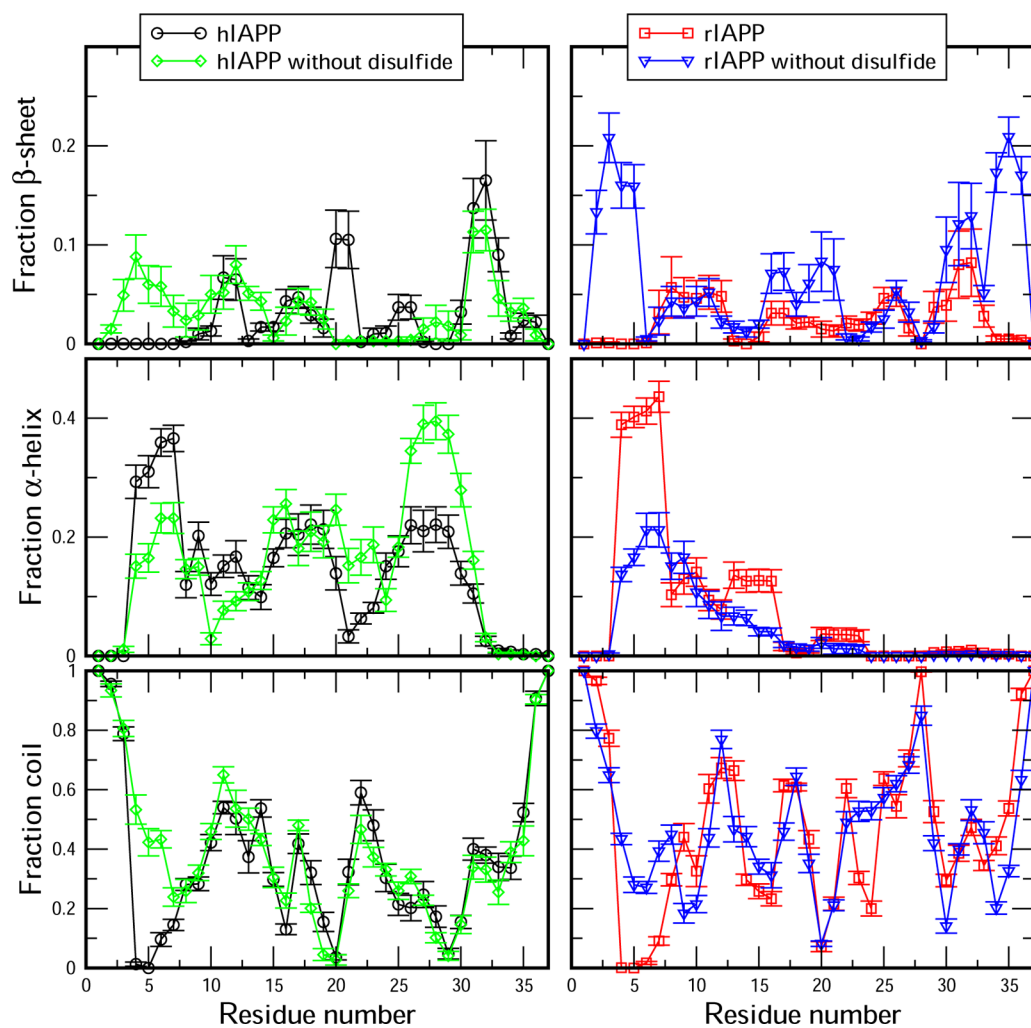


Figure 9. Per-residue fraction of time spent in secondary structure over the last 150 ns for wild-type hIAPP and rIAPP, as well as both hIAPP and rIAPP without the disulfide bond.